Refined proper motions of some high-velocity stars

S. V. Zhuiko*and A. K. Dambis†

[1] *Sternberg Astronomical Institute,*
M.V.Lomonosov Moscow State University,
Universitetskii pr. 13, Moscow, 119991 Russia

Abstract – .
Key words: hypervelocity stars.

Short introduction to subject of the paper ...

1 Introduction

The first hypervelocity star was discovered by Warren Brown in 2005 by analyzing the results of a spectroscopic survey performed with the MMT telescope. Brown et al. (2005) found a $3M_{\odot}$-mass main-sequence B-type star moving at a Galactocentric velocity of 700 km/s, which is equal to twice the escape velocity at a Galactocentric distance of 100 kpc. The existence of such stars was predicted by Jack Hills (Hills, 1988). The discovery of the first hypervelocity star triggered a great interest in the Hills concept, which had been lying idle for about two decades. When asked about the discovery, Hills responded that it was high time someone found it (Perlman, 2005). There are a lot of mechanisms for accelerating stars to high

*E-mail: navigator@sai.msu.ru
†E-mail: dambis@yandex.ru

velocities, e.g., those suggested by Tutukov & Fedorova (2009), however, the Hills mechanism is unique in its capability to accelerate large numbers of main-sequence stars. Hence main-sequence stars are among the hypervelocity star candidates. They can be accelerated and ejected from any galaxy hosting a supermassive black hole at its center. There are several definitions of hypervelocity stars (Brown, 2015). According to Brown's definition, main-sequence stars originating from the Galactic center are referred to as hypervelocity stars, and those that escape from the Galactic disk are referred to as hyper-runaway stars.

The Milky Way hosts more than 2×10^{11} gravitationally bound stars and a certain number of gravitationally unbound stars with positive energy in the Galactic gravitational field. These stars emerge from the Galactic center, move into the dark halo along straight-line trajectories, and escape from the Galaxy. Hereafter we denote then as HVS. To kinematically test the hypothesis that they originate in the Galactic center we have to determine their current space velocities. Unfortunately, the angular displacements of these stars in the sky are negligible and determining space trajectories of HVSs with the most advanced ground-based telescopes would require several decades. However, the publication of the second release of the Gaia catalog (Gaia Collaboration et al. 2018) provided proper-motion measurements of unprecedented accuracy to complement the radial velocities measured with the 6.5- and 8.1-m telescopes. The Gaia satellite produced the most complete and accurate catalog of Milky-Way stars with astrometric parameters for more than 1 billion objects. However, the mass and distance range spanned by the Gaia sample differ from those of non-Gaia stars represented by (2.5-4)$M_{\odot}$-mass stars in the dark halo (Irrgang et al., 2018). An analysis of combined data will help determine the origin of HVSs, confirm or disprove their hypervelocity status, and make it possible to refine the Galactic potential model (Gnedin et al., 2005; Kenyon, 2008; Kenyon, 2014; Contigiani et al., 2018).

The star HD 271791 is the first example of a so-called hyper-runaway star ejected from the disk in the direction of Galactic rotation. Hereafter we denote such stars by the HRS acronym. Note, for the sake of fairness, that the term "runaway" was proposed by Adrian Blaauw (Blaauw, 1961). Runaway stars appear when a $55M_{\odot}$ component in the former massive binary explodes as a supernova. In the case of certain combinations of the parameters of the binary the second component acquires high space velocity and, after the binary disrupts as a result of the supernova explosion (Poveda et al., 1967).

HRS can be confused with a HVS if its velocity is equal to 400 km/s. The Milky-Way potential model shows that HRS moving at velocities no greater than 400 km/s in the $10 < \mathrm{RGC} < 20$ kpc domain are gravitationally bound. Another formation mechanism of HRSs is provided by the Gvaramadze scenario (Gvaramadze et al., 2009), which consists in a component of a close binary being ejected in the direction of Galactic rotation by very massive stars residing in young open clusters in Galactic spiral arms.

The main hypothesis of the origin of HVS assumes that they form as a result of Hills scenario - dynamic ejection of a star from the Galactic center. The existence of HVS in the Galaxy is a natural consequence of the presence of a central supermassive black hole (SMBH) with a mass of $(4.31 \pm 0.06) \times 10^6 M_\odot$ surrounded by the central star cluster with a total stellar mass of greater than $10^6 M_\odot$. Ejection occurs as a result of dynamic triple interaction of close $m_a + m_b$ binaries with semimajor axis a_{bin}, AU, when such a binary approaches the SMBH to the distance R_{close}:

$$R_{close} \sim (30 - 200)(a_{bin}/(1AU)), AU \tag{1}$$

One of the components of the binary becomes captured into an elliptic orbit with the SMBH located at the active focus of the ellipse, whereas the second component is ejected at a high space velocity and becomes a HVS. Stars captured into stationary orbits the so called S-stars are B-type main-sequence stars (Fig. 1).

The smaller R_{close}, the higher is the HVS ejection velocity (Fig. 2). The maximum ejection velocity in Hill's scenario is limited by tidal destruction (Dremova et al., 2015). When one of the components approaches the SMBH to a distance of R_{tidal}, it is gradually destroyed by tidal forces:

$$R_{tidal} \sim a_{bin}(3M_{BH}/(m_{HVS} + m_S))^{(1/3)} \times (r/R_\odot), AU, \tag{2}$$

where M_{BH} is the mass of the SMBH in $M\odot$, and $R\odot$ is the solar radius in AU.

The ejection of a HVS was modeled in numerical simulations the so-calle scenario of Yu and Treimaine (Yu & Tremaine, 2003; Sesana et al., 2007). Stars can be accelerated to velocities of 10^4 km/s as a result of dynamical friction between a system of two supermassive black holes with the total mass of $10^6 M\odot$ to $10^9 M\odot$ and bulge stars. This process should cause the variation of the parameters of stellar orbits followed by the ejection of the HVS. Radiation of gravitational waves causes the intermediate-mass black hole (IMBH)

to spiral toward the SMBH (the so-called IMBH spiraling event). However, a single IMBH spiraling eventtakes, on the average, a HVS get to the dark halo from the Galactic center, and therefore this scenario requires several IMBH spiraling events to explain the observed number of HVSs.

Merritt et al. (2009) and Merritt (2010, 2013) showed that an IMBH orbiting the SMBH at the center of the Milky Way may effectively randomize the distribution of stars near the SMBH transforming the initially thin rotating stellar disk into almost isotropic distribution of stars moving around the SMBH in orbits with chaotically distributed eccentricities. This process takes 1 Myr, i.e., less than the stellar evolutionary time scales provided that the IMBH mass exceeds $1500 M\odot$ and the orbital eccentricity of the IMBH is 0.5 or higher. The final distribution of the semimajor axes of stellar orbits depends in the assumed mass of the IMBH, however, stars with apocentric distances no less than the pericenter of the IMBH orbit are generated most efficiently. The IMBH formation rate is estimated to be $10 - - 7 \times yr^{--1}$ in terms of a semianalytical model of the formation and evolution of clusters in the Galactic center. Black holes merge and the process repeats. This is one of the possible explanations of the paradox of the young age of S-stars. The IMBH randomizes the S-star distribution before the merger with the SMBH. Thus this model does not necessarily imply that an IMBH is now actually present in the cluster of S-stars.

Although the presence of another IMBH in the Galactic center is open to doubt (orbits of S-stars are unperturbed), this possibility cannot be completely ruled out. Note that the existence of binary black holes in other galaxies can be considered an established fact (Kormendy & Ho, 2013). Numerical simulations showed that encounters of stars with supermassive binary black holes in galactic nuclei result in the formation of HVSs (Zhuiko et al., 2017).

The formulation of the three-body problem in terms of the modified Hills scenario allows dynamic capture of a binary consisting of the parent IMBH and a single star by the gravitational field of the more massive SMBH. Simulations predict the existence of stars with space velocities comparable to the speed of light (Dremova et al., 2017). Let us denote them by the RVS (relativistic-velocity stars) acronym.

Table 1: Comparison of HVS properties.

Mass of HVSs:	2.5–3.0$M_{\odot}$
Spectral type:	B9
Travel time:	t_{trvl} ∼60–200 Myr
Probability of HVS formation:	(2–8)×10^{--5} yr^{--1}
Mass of S-stars:	M ≥ 5 M⊙
Main-sequence lifetime of S-stars:	$t_{MS} \sim$ 100 Myr
Probability of S-stars formation:	(1–4)×10^{--5} yr^{--1}
Runaway stars (RAS):	50–100 km/s
Hyper-runaway stars (HRS):	100–400 km/s
Hypervelocity stars (HVSs):	400–1200 km/s
Relativistic-velocity stars (RVS):	> 30000 km/s

2 Refining the proper motions

For most of the known high-velocity stars Gaia DR2 (Gaia Collaboration 2018) provides proper motions of unprecended accuracy, which can hardly be improved by any significant amount. However, the proper-motion errors increase rapidly at the faint end of the Gaia DR2 magnitude distribution ($G_{mag} \geq 19.0^m$), reaching 1 mas/yr or more for the faintest stars. The Gaia DR2 proper motions of these stars can potentially be improved by taking into account positional data from other surveys with sufficient positional accuracy and appreciable epoch difference from 2015.5. An analysis of the currently publicly available large-scale sky catalogs showed that the most promising survey candidates are SDSS (Paris et al. 2018) (observing epochs about 2001, implying an epoch difference with Gaia DR2 of ∼ 15 years), PanStarrs (Chambers wt al. 2016) (observing epochs about 2011, implying an epoch difference with Gaia DR2 of ∼ 4 years), and UKIDSS (Lawrence et al. 2007) (observing epochs about 2008, implying an epoch difference with Gaia DR2 of ∼ 7 years). Here we try to refine the Gaia DR2 proper motions for nine hypervelocity stars from the Open Fast Star Catalog (Boubert et al. 2018) with the Gaia DR2 total proper-motion errors $(\sigma(\mu_\alpha)^2 + \sigma(\mu_\delta)^2)^{1/2} \geq 1.5$ mas/yr. We start by cross-matching stars in Gaia DR2, SDSS, PanStarrs, and UKIDSS surveys within 5 arcmin from the target star with a cross-match radius of 2 arcsec. We then use Gaia DR2 as the reference catalog to define the frame to which we reduce the star positions from the other three catalogs via standard linear (6-constant) procedure (we ignore higher-order terms be-

Table 2: Parameters of HVSs.

Name	RA	DEC	V_r km/s	Distance, kpc	PM_{RA} mas/yr	PM_{DEC} mas/yr	V_r/dist references*
HVS22	175.443518	4.704796	597.8	84.36	2.440 ± 1.356	0.911 ± 1.283	1/4
LMST-HVS26	103.649037	17.054187	307.0	0.2	6.141 ± 0.861	-13.616 ± 1.272	2/2
SDSSJ074256.45+275946.9	115.735261	27.996373	28.6	11.44	0.569 ± 1.140	0.075 ± 0.809	3/5
SDSSJ085508.03+031505.4	133.783462	3.251498	54.7	13.56	-0.116 ± 1.206	-0.895 ± 0.697	3/5
J154556.10+243708.9	236.483739	24.619116	193.0	85.05	0.153 ± 0.964	-0.328 ± 1.087	1/9
SDSSJ053553.15+004051.6	83.971484	0.680988	-5.9	2.41	0.826 ± 1.003	0.494 ± 1.176	3/5
SDSSJ072331.00+374628.2	110.879210	37.774511	-26.1	10.94	0.554 ± 0.969	1.167 ± 0.624	3/5
SDSSJ023849.85+281023.6	39.707734	28.173200	-71.6	8.98	-1.032 ± 0.536	0.860 ± 1.064	3/5
SDSSJ092613.29+201253.0	141.555401	20.214739	76.8	5.31	-0.027 ± 0.493	-0.264 ± 0.863	3/5

* V_r and distance references: 1. Smith et al. (2010); 2. Zhong et al. (2014); 3. Boubert et al. (2018) 4. Brown et al. (2014); 5. Alam et al. (2015); 6. Brown et al. (2009)

cause of the small size of the 5-arcmin-radius area) along the lines described in Klinichev et al. (2018). We then infer the proper-motion components via least squares method and, finally, compute the weighted average of the proper-motion value so inferred and the Gaia DR2 proper motion and adopt this estimate as our refined proper motion.

The results are listed in Table2. Its columns give: column (1), the name of the star; columns 2 and 3, the Gaia DR2 equatorial coordinates (epoch 2015.5); column 4, the radial velocity in km/s; column 5, the heliocentric distance in kpc; columns 6 and 7, the refined PM_{RA} and PM_{DEC} proper-motion components in mas/yr, and column 8, the radial-velocity/distance references. Figs. 1 and 2 illustrate this procedure in the case of the star SDSSJ085508.03+031505.4. Figs. 1 and 2 show the quantities $\Delta\alpha\times cos\delta = (\alpha - \alpha_{Gaia}) \times cos\delta$ and $\Delta\delta = (\delta - \delta_{Gaia})$ (both in arcsec) plotted as a function of time. The slopes of the corresponding linear least-squares fits (the dashed lines) give the estimates μ_α and μ_δ of the components of the proper motion of the star. The final estimates $\mu_\alpha(Final)$ and $\mu_\delta(Final)$ listed in Table 2 are computed as the weighed averages of these μ_α and μ_δ values and the corresponding values provided in Gaia DR2, $\mu_\alpha(GaiaDR2)$ and $\mu_\delta(GaiaDR2)$.

3 Orbits

3.1 Galactic potential model

In this paper we use an axisymmetric model gravitational potential of the Galaxy represented by three components: the Miyamoto and Nagai (1975) disk , Hernquist spheroid (Hernquist 1990), and modified isothermal dark-

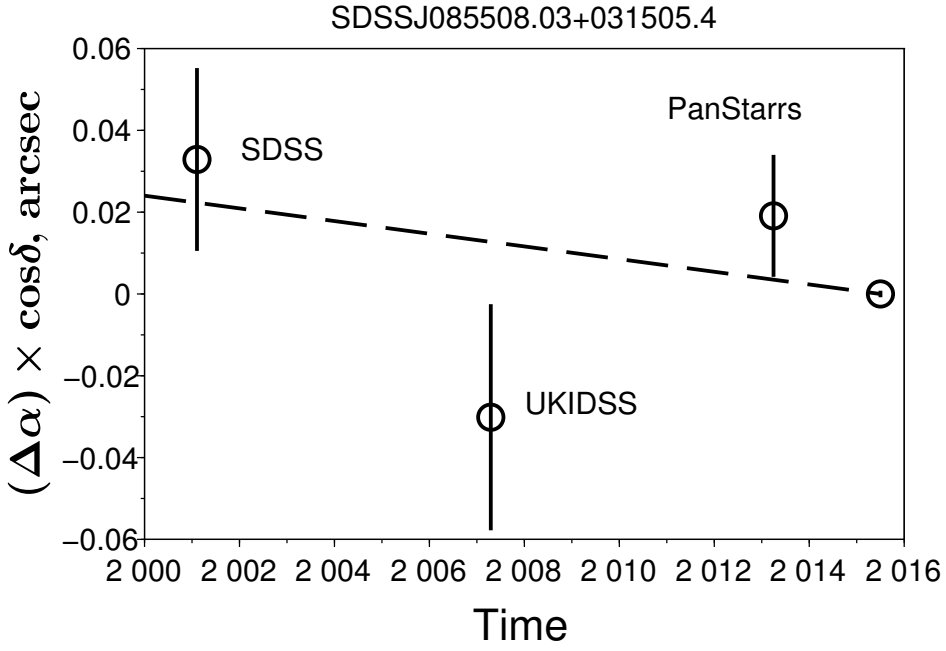

Figure 1: The offset of the SDSS, UKIDSS, and PanStarrs catalog positions of the star SDSSJ085508.03+031505.4 along the right ascension direction reduced to Gaia DR2 frame with respect to its Gaia DR2 2015.0 position, $\Delta\alpha \times cos\delta = (\alpha - \alpha_{GaiaDR2}) \times cos\delta$, plotted as a function of time. The dashed line shows the least-squares fit used to estimate the proper motion component μ_α. The final estimate $\mu_\alpha(Final)$ is computed as the weighed average of this μ_α value and the value provided in Gaia DR2

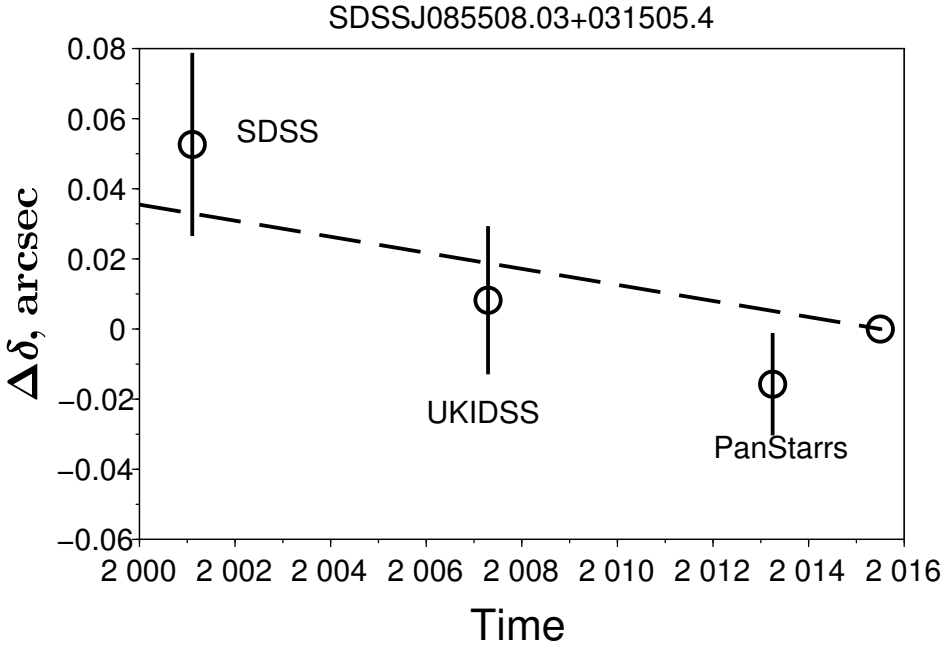

Figure 2: The offset of the SDSS, UKIDSS, and PanStarrs catalog positions of the star SDSSJ085508.03+031505.4 along the declination direction reduced to Gaia DR2 frame with respect to its Gaia DR2 2015.0 position, $\Delta\delta = (\delta - \delta_{GaiaDR2})$, plotted as a function of time. The dashed line shows the least-squares fit used to estimate the proper motion component μ_δ. The final estimate $\mu_\delta(Final)$ is computed as the weighed average of this μ_δ value and the value provided in Gaia DR2

matter halo. The formulas for the potentials of these three components have the following form:

$$\phi_{disk} = -\frac{GM_{disk}}{\sqrt{R^2 + \left(a + \sqrt{z^2 + b^2}\right)^2}} \tag{3}$$

$$\phi_{spher} = -\frac{GM_{spher}}{\sqrt{R^2 + z^2} + c} \tag{4}$$

$$\phi_{halo} = V_{halo}^2 \ln\left(R^2 + z^2 + d^2\right) \tag{5}$$

Fig. 3 shows the Galactic rotation curve corresponding to this potential.

3.2 HVS orbits

We integrated the orbits of nine HVS objects from Table 2 for 10 Gyr forward. Most of the stars move in rossette-shaped orbits (see Fig. 4 as an example) with the important exceptions of J154556.10+243708.9, which moves in a highly elongated loop-like orbit reaching a maximum Galacticentric distance of 543 kpc (see Fig. 6), and HVS22, which appears to be escaping the Galaxy at a high velocity of 910 km/s.

4 Conclusions

We refined the Gaia DR2 proper motions of nine high-velocity stars with Gaia DR2 total proper-motion errors $\sigma\mu \geq 1.5$ mas/yr and computed the Galactic orbits of these objects. The total errors of our refined proper motions range from 1 to 1.9 mas/yr compared to 1.4 to 2.5 mas/yr for the initial Gaia DR2 proper motions. Our proper-motion errors translate into transversal velocity errors ranging from 0.3 to 160 km/s compared to determined accurate absolute proper motions (with a typical accuracy of ~ 0.4 mas/yr, which translates into a ~ 17 km/s transversal-velocity error) and computed Galactic orbits for the currently largest sample of Galactic globular clusters (115 objects), which represents a two-fold increase compared to the most extensive previous studies. We computed the cluster orbits in terms of both an axisymmetric potential model and a model with a rotating bar. Unlike what

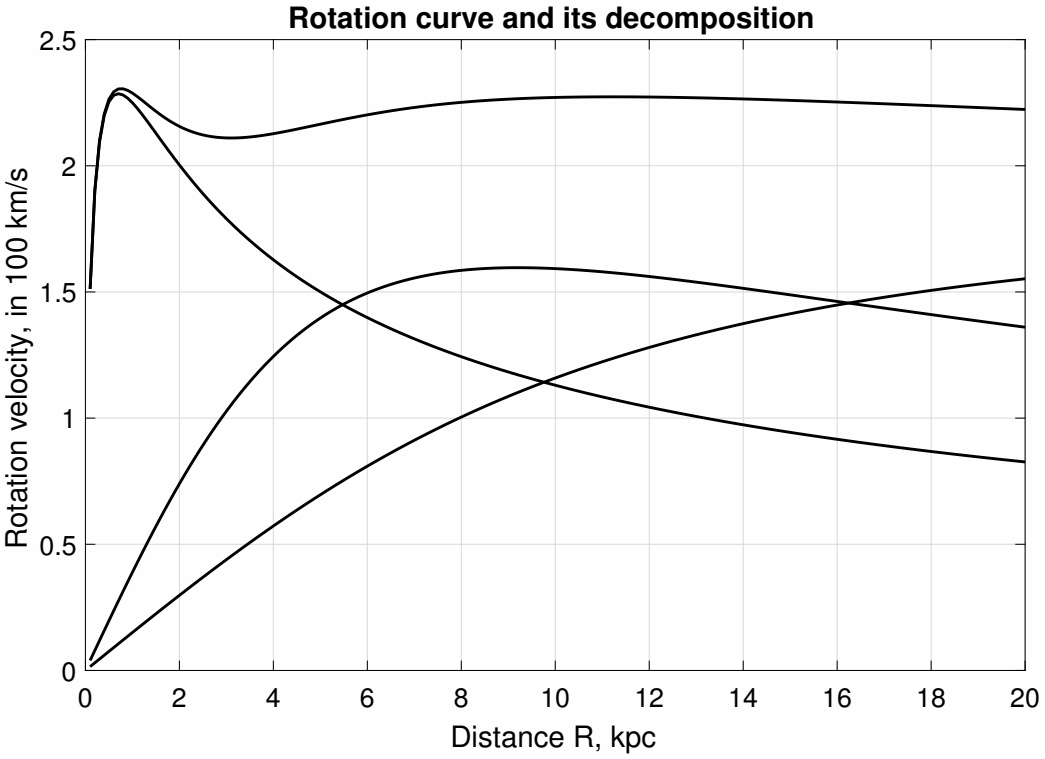

Figure 3: Decomposition of the rotation curve based on the adopted Galactic gravitational potential (see text)

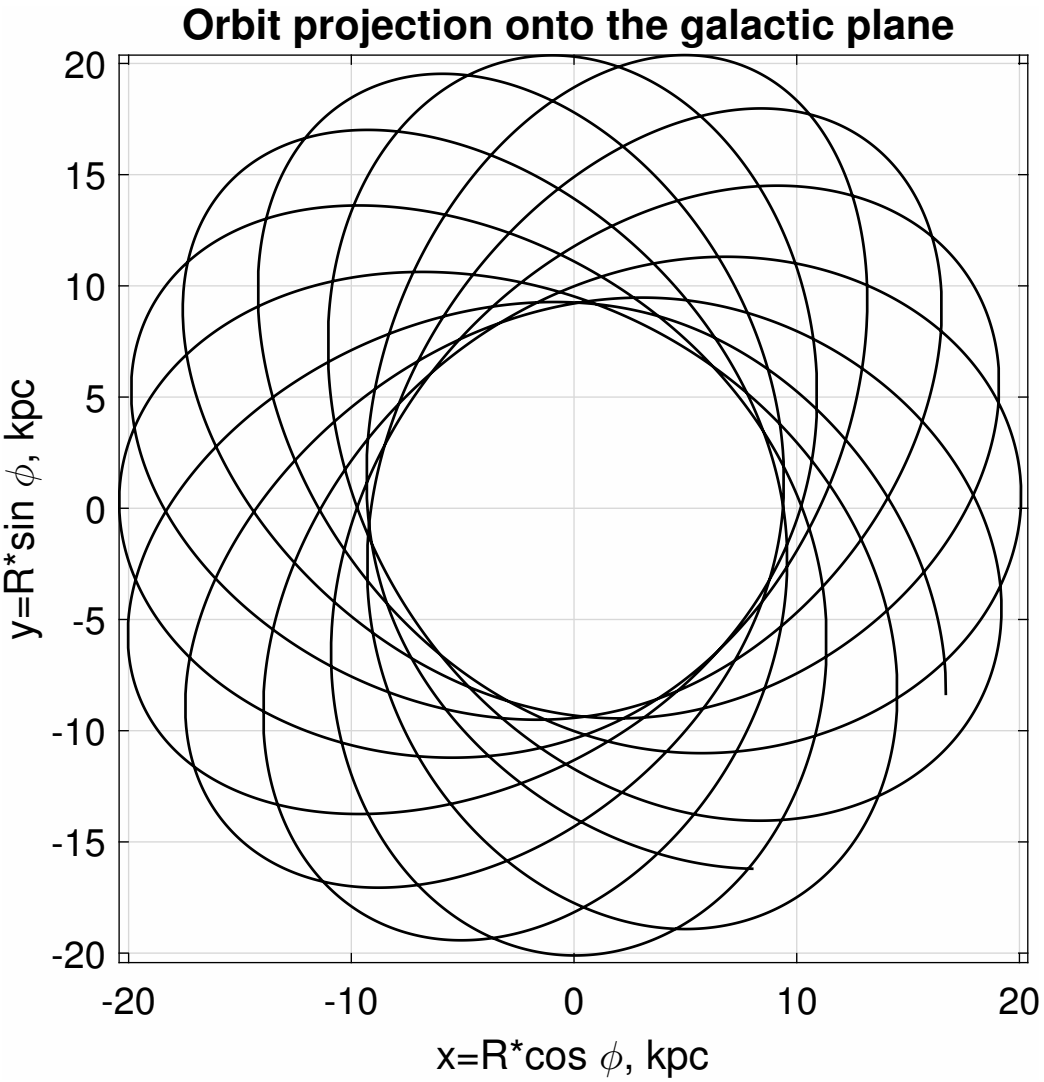

Figure 4: Galactic-plane projection of the rosette-shaped orbit of the star SDSSJ085508.03+031505.4

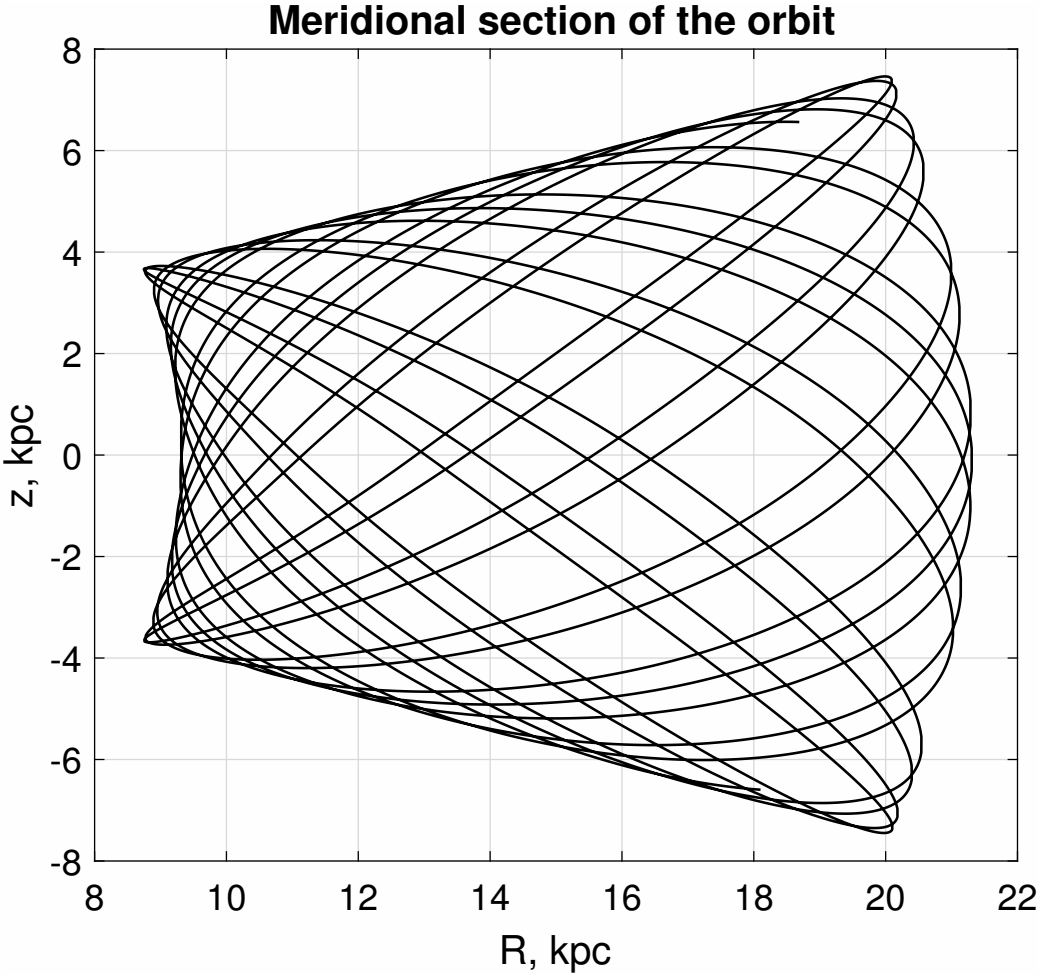

Figure 5: Meridional section of the orbit of the star SDSSJ085508.03+031505.4

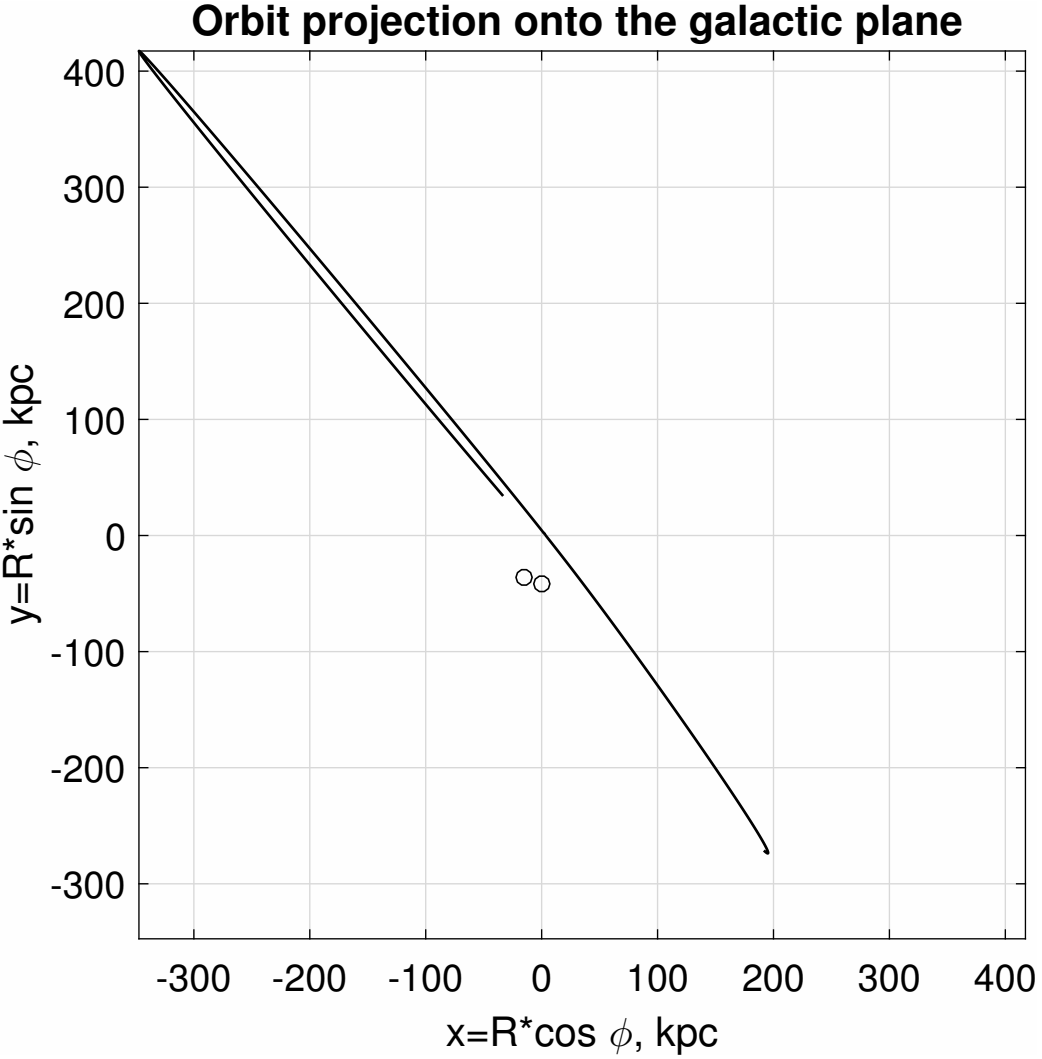

Figure 6: Galactic-plane projection of the rosette-shaped orbit of the star SDSSJ085508.03+031505.4

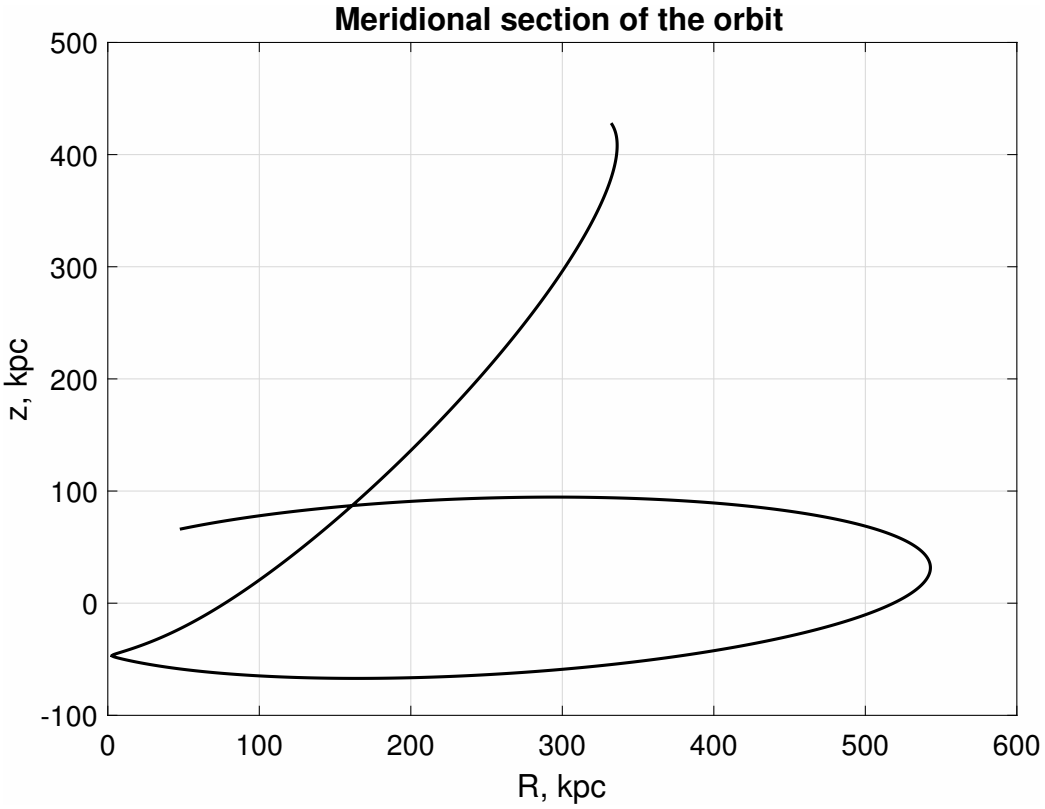

Figure 7: Meridional section of the orbit of the star SDSSJ085508.03+031505.4

was found by the authors of earlier studies, we conclude that the bar has appreciable effect on the orbits of practically all clusters in that it randomizes the orbits and especially their portions in the vicinity of the Galactic center, and stretches out the orbits of some of the thick-disk clusters.

ACKNOWLEDGEMENTS

This work has made use of data from the European Space Agency (ESA) mission *Gaia* (`https://www.cosmos.esa.int/gaia`), processed by the *Gaia* Data Processing and Analysis Consortium (DPAC, `https://www.cosmos.esa.int/web/gaia/dpac/consortium`). Funding for the DPAC has been provided by national institutions, in particular the institutions participating in the *Gaia* Multilateral Agreement. This work was supported by the Russian Foundation for Basic Research (grant no. 18-02-00890).

References

Alam S. et al. (2015) ApJS 219, 12
Blaauw A. (1961) Bull. Astron. Inst. Netherlands, 15, 265
Boubert D., Guillochon J., Hawkins K., Ginsburg I., Evans N. W., Strader J. (2018) MNRAS 479, 2789
Brown W. R., Geller M. J., Kenyon S. J., Kurtz M. J. (2005) ApJ, 622, L33
Brown W. R., Geller M. J., Kenyon S. J. (2009) ApJ, 690, 1639
Brown W. R., Geller M. J., Kenyon S. J. (2014) ApJ 787, 89
Brown W. R. (2015) ARA&A, 53, 15
Chambers et al. (2016) arXiv161205560
Contigiani O., Rossi E. M., Marchetti T. (2018) MNRAS 476, 4697
Dremova G. N., Dremov V. V., Orlov V. V., Tutukov A. V., Shirokova K. S., (2015) Astron. Rep. 59, 1019 [AZh, 92, 907]
Dremova G. N., Dremov V. V., Tutukov A. V. (2017) Astron. Rep. 61, 573 [AZh 94, 580]
Gaia Collaboration, A. G. A. Brown, A. Vallenari, et al. (2018) arXiv1804.09365
Gnedin O. Y., Gould A., Miralda-Escude J., Zentner A. R. (2005) ApJ 634, 344
Gvaramadze V., Gualandris A., Portegies Zwart S. (2009) MNRAS 396, 570
Hernquist L. (1990) AJ 356, 359
Hills J. G. (1988) Nature 331, 687
Irrgang A., Kreuzer S., Heber U., Brown W. (2018) A&A 615, L5

Kenyon S. J. et al. (2008) ApJ 680, 312
Kenyon S. J. et al., (2014) ApJ 793, 122
Klinichev A.D., Glushkova E. V., Dambis A. K., and Yalyalieva L. N., (2018) Astron. Rep., in press.
Kormendy J, Ho L.C. (2013) Ann. Rev. Astron. Astrophys. 51, 511
Miyamoto M. and Nagai R., (1975) PASJ 27, 533
Laurence A. (2007) MNRAS 379, 1599
Lu Y., Zhang F., Yu Q. (2010) ApJ 709, 1356
Merritt D., Gualandris A., Mikkola S. (2009) ApJ 693, L35
Merritt D. (2010) ApJ 718, 739
Merritt D. (2013) Dynamics and evolution of Galactic nuclei. Princeton U. Press
Paris, I., Petitjean, P., Aubourg, E., et al. (2018) A&A, 613, A51
Perlman D. (2005) Wandering star screaming from Milky Way/runaway youngster clocked at more than 1.5 million mph. San Francisco Chronicle, Feb. 11
Poveda A., Ruiz J., Allen C. (1967) Bol. Obs. Tonantzintla Tacubaya 4, 860
Sesana A., Haardt F., Madau P. (2007) ApJ 660, 546
Smith K. W., Bailer-Jones C. A. L., Klement R. J., Xue X. X. (2010) A&A 522, 88
Tutukov A.V., Fedorova A.V. (2009) Astron. Rep. 53, 839
Yu Q., Tremaine S., (2003) ApJ 599, 1129
Zhong Jing et al. (2014) ApJ 789, L2
Zhuiko S. V., Orlov V. V., Shirokova K. S., (2017) Astron.Rep. 61, 47 [AZh 94, 53]